Insertion of Imine into Palladium−Methyl and Palladium−Acyl Bonds. A Density Functional Study

Luigi Cavallo

Contribution from the Dipartimento di Chimica, Università di Napoli Via Mezzocannone 4, I-80134 Napoli, Italy

Received November 25, 1998. Revised Manuscript Received February 24, 1999

Abstract: The insertion mechanism of imine into the Pd−methyl and Pd−acyl bonds with a phosphane or a nitrogen-based ligand coordinated to the Pd atom has been studied with density functional theory. In agreement with the experimental findings, σ coordination of the imine is preferred. Imine insertion into the Pd−methyl bond presents high energy barriers (>40 kcal mol^{-1}) independently of the Pd-ligand used. On the contrary, insertion into the Pd−acyl bond is more facile, with energy barriers close to 20 kcal mol^{-1}. A geometrical and energetic analysis of the transition states suggests that the formation of the very strong amide linkage constitutes the added driving force for the imine insertion into the Pd−acyl bond.

1. Introduction

The palladium-catalyzed insertion of unsaturated molecules into Pd−carbon bonds has received remarkable attention over the last years, and alkenes and alkynes have been shown to be particularly prone to insert into the Pd−carbon bond.[1] This aptitude for insertion reactions (and hence carbon−carbon bond formation) has been extended to the polymerization of α-olefins.[2] Moreover, copolymerization of alkenes with carbon monoxide is a currently active area of research,[3−6] and theoretical investigations contributed to a deep understanding of the mechanisms of insertion into the Pd−alkyl and Pd−acyl bonds.[7,8]

In contrast to the facile insertion of alkenes, insertion of molecules with multiple carbon−nitrogen bonds, particularly imines, is not as common and easy.[9−11] In fact, the first direct insertion of imines into transition metal−carbon bonds was only recently independently reported by Arndtsen and Sen.[12,13] Several cationic L_2Pd^{II}(methyl)(imine) complexes were obtained by Arndtsen (L_2 = 2,2′-bipyridyl ligand) and Sen (L_2 = bidentate phosphane and nitrogen-donor based ligands). These imine complexes were found to be very stable, and no evidence of imine insertion into the Pd−methyl bond was observed. ^{1}H and ^{13}C NMR investigations clearly indicated that the imino ligand was bound to the Pd atom by σ donation of the nitrogen lone pair, and that π complexation of the imine could be excluded.[12,13] In a subsequent reaction, the investigated L_2Pd^{II}(methyl)(imine) complexes reacted with carbon monoxide to form the corresponding L_2Pd^{II}(acyl)(imine) complexes. Insertion of the imine into the Pd−acyl bond occurred at room temperature, resulting in the formation of an amido group.[12,13] IR and X-ray investigations, as well as ^{31}P and ^{1}H NMR experiments, indicated that the oxygen carbonyl atom was coordinated to the Pd atom to form a stable 5-membered ring.

The discovery of this method for the formation of carbon−nitrogen bonds could represent a first step toward a possible new route for the synthesis of polypeptides. For this reason, we studied the imine insertion into the Pd−carbon bond of the complexes $L_2Pd^{II}R^+$ (L_2 = $H_2PCH_2CH_2PH_2$ or HN═CH−CH═NH, R = CH_3 or C(═O)CH_3) with gradient corrected density functional theory to shed light on the main features of these mechanisms. The two considered Pd ligands, $H_2PCH_2CH_2PH_2$ and HN═CH−CH═NH, mimic the basic skeleton of the phosphane and bipyridyl ligands used by Sen and Arndtsen, respectively.

2. Computational Details

The density functional calculations were carried out by using the ADF package developed by Baerends et al.[14−16] The geometry optimization procedure has been developed by Versluis and Ziegler.[17] The electronic configurations of the molecular systems were described by an uncontracted triple-ζ STO basis set on Pd (4s, 4p, 4d, 5s, 5p).[18] Double-ζ STO basis sets were used for P (3s, 3p), O (2s, 2p), N (2s, 2p), C (2s, 2p), and H (1s).[18] These basis sets were augmented with single 3d and 2p polarization functions for the P, O, N, C, and H atoms, respectively.[18] The $1s^22s^22p^63s^23p^63d^{10}$ configuration on Pd, the $1s^22s^22p^6$ on P, and the $1s^2$ on O, N, and C were treated by the frozen-core approximation. The calculations have been performed by using

(1) Collman, J. P.; Hegedus, L. S.; Norton, J. R.; Finke, R. G. *Principles and Applications of Organotransition Metal Chemistry*; University Science Books: Mill Valley, CA, 1987.
(2) Johnson, L. K.; Killian, C. M.; Brookhart, M. S. *J. Am. Chem. Soc.* **1995**, *117*, 6414.
(3) Drent, E.; Budzelaar, P. H. M. *Chem. Rev.* **1996**, *96*, 663.
(4) Jiang, Z.; Sen, A. *J. Am. Chem. Soc.* **1995**, *117*, 4455.
(5) Rix, F. C.; Brookhart, M.; White, P. S. *J. Am. Chem. Soc.* **1996**, *118*, 4746.
(6) Sen, A. *Acc. Chem. Res.* **1993**, *26*, 303.
(7) Margl, P. M.; Ziegler, T. *Organometallics* **1996**, *15*, 5519.
(8) Margl, P. M.; Ziegler, T. *J. Am. Chem. Soc.* **1996**, *118*, 7337.
(9) Müller, F.; van Koten, G.; Vrieze, K.; Heijdenrijk, D. *Organometallics* **1989**, *8*, 33.
(10) Reduto dos Reis, A. C.; Hegedus, L. S. *Organometallics* **1995**, *14*, 1586.
(11) Vasapollo, G.; Alper, H. *Tetrahedron Lett.* **1988**, *29*, 5113.
(12) Dghaym, R. D.; Yaccato, K. J.; Arndtsen, B. A. *Organometallics* **1998**, *17*, 4.
(13) Kacker, S.; Kim, J. S.; Sen, A. *Angew. Chem., Int. Ed. Engl.* **1998**, *37*, 1251.
(14) ADF 2.3.0; Vrije Universiteit Amsterdam: Amsterdam, The Netherlands, 1996.
(15) Baerends, E. J.; Ellis, D. E.; Ros, P. *Chem. Phys.* **1973**, *2*, 41.
(16) te Velde, B.; Baerends, E. J. *J. Comput. Phys.* **1992**, *99*, 84.
(17) Versluis, L.; Ziegler, T. *J. Chem. Phys.* **1998**, *88*, 322.
(18) Snijders, J. G.; Vernooijs, P.; Baerends, E. J. *At. Nucl. Data Tables* **1981**, *26*, 483.

10.1021/ja9840706 CCC: $18.00
Published on Web 04/14/1999

the local exchange-correlation potential by Vosko et al.,[19] augmented by Becke's[20] gradient exchange correction and by Perdew's[21,22] gradient correlation correction also during the geometry optimizations. First-order scalar relativistic corrections were added to the total energy.

The transition state geometries were approached by a linear-transit procedure using the N−C (methyl or acyl) distance as the reaction coordinate, while optimizing all other degrees of freedom. Full transition state searches were started from geometries corresponding to maxima along the linear-transit curves. Frequencies were calculated to characterize the obtained transition state geometries with the phospane ligand. Only one negative frequency was found for imine insertion into both the Pd−C(methyl) and Pd−C(acyl) bonds. The computationally expensive frequency calculations were not performed on the transition state geometries with the nitrogen-based ligand since they are substantially similar to the transition state geometries with the phospane ligand.

3. Results and Discussion

Coordination of the imine into the free apical position of the phosphane-based Pd−methyl and Pd−acyl imine free species (**1aP** and **1bP**, respectively) occurs in a barrierless fashion and led to the imine σ-coordinated square-planar species **2aP** and **2bP**, respectively. In the following, a capital **P** or **N** attached to a species label denotes a species containing the H_2PCH_2-CH_2PH_2 or the HN═CH−CH═NH ligand, respectively. The imine uptake energy to **1aP** and **1bP** is equal to −37.2 and −27.8 kcal mol^{-1}, respectively. The lower uptake energy for **1bP** is due to the rupture of the stabilizing η^2 interaction of the C═O group with the Pd atom.[8] We also tried to optimize a geometry with a π-coordinated imine both for the Pd−methyl and Pd−acyl species. All attempts inevitably converged into **2aP** and **2bP**, suggesting that the π-coordinated imine does not represent a minimum.[23]

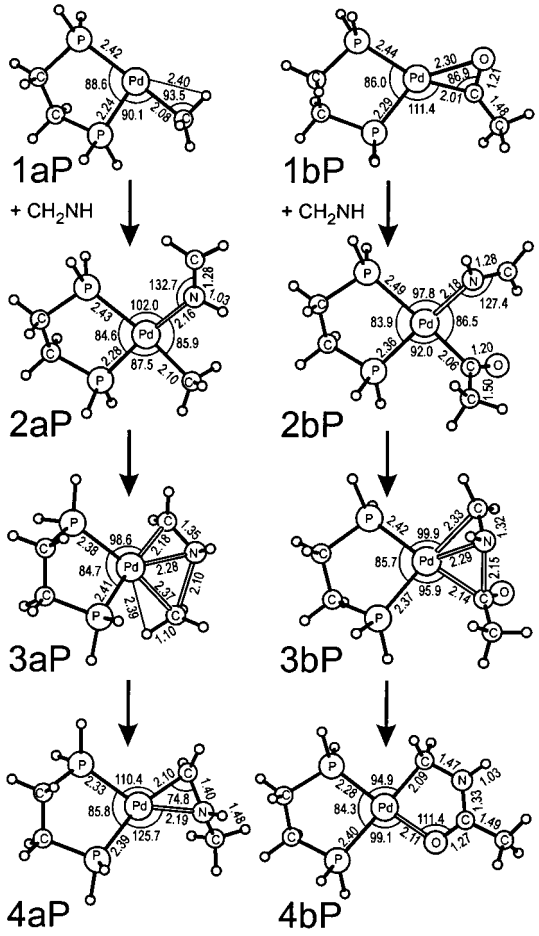

Insertion of the imine into the Pd−methyl and Pd−acyl bonds was modeled by contraction of the distance between the nitrogen atom and the carbon atom of the methyl group or of the carbonyl group, respectively. Only in the last stages of the path from **2aP** and **2bP** toward the transition state does the imine reorient itself to an almost π coordination. A full transition state search led to **3aP** and **3bP**, respectively, which are geometrically similar to those structures encountered in the ethene insertion into the Pd−alkyl and Pd−acyl bonds by Margl and Ziegler.[8] Structures **3aP** and **3bP** lie 42.4 and 18.9 kcal mol^{-1}, respectively, above the σ-coordinated imine complexes **2aP** and **2bP**, respectively. The very high barrier found for insertion into the Pd−methyl bond is in agreement with the experimentally observed great kinetic stability of the L_2Pd(methyl)(imine) complexes.[13] The calculated barrier for insertion into the Pd−acyl bond, instead, is slightly higher than the barrier experimentally determined by Brookhart and co-workers for insertion of ethene into the Pd−acyl bond of an analogous Pd complex (16.6 kcal mol^{-1}),[5] and than the barrier calculated for insertion of ethene into the Pd−acyl bond (13.9 kcal mol^{-1}).[8] Relaxation of the transition states **3aP** and **3bP** led to the products **4aP** and **4bP**, respectively. The sp^3 nitrogen atom of **4aP** is severely bent toward the Pd atom, and it is strongly coordinated to the metal through the lone pair. On the other hand, the carbonyl oxygen of **4bP** is bonded to the metal and closes a five-membered ring, in agreement with the experimental results,[13] and as is common for closely related species.[8,12,24] The overall reactions **2aP** → **4aP** and **2bP** → **4bP** are exothermic with enthalpies of −13.0 and −21.6 kcal mol^{-1}, respectively.

It is worthy to note that the geometries of **3aP** and **3bP** suggest they correspond to a late and to an early transition state, respectively. In fact, the Pd−C bond which is going to be broken is 13% stretched in **3aP** relative to **2aP**, whereas it is only 4% stretched in **3bP** relative to **2bP**. Moreover, the C−N bond that is going to be formed is 42% longer in **3aP** relative to **4aP**, whereas it is quit longer, 62%, in **3bP** relative to **4bP**. That is, the Pd−C bond that is going to be broken is quite a bit closer to the reactants in **3bP**, while the C−N bond that is going to be formed is quite a bit closer to the products in **3aP**.

To determine the origin of the lower barrier for insertion into the Pd−acyl bond, we fragmented the structures of the reactants **2aP** and **2bP** and of the transition states **3aP** and **3bP** into three pieces, $L_2Pd\bullet^+$, R• (R• = •CH_3, •C(═O)CH_3), and CH_2NH, while retaining all their geometric parameters. Starting from these rigid fragments, the reactants **2aP** and **2bP** and the transition states **3aP** and **3bP** were recomposed in the following way,

$$L_2Pd\bullet^+ + R\bullet \rightarrow L_2Pd{-}R^+ \qquad \text{(I)}$$

and

$$L_2Pd{-}R^+ + CH_2NH \rightarrow L_2Pd{-}R(CH_2NH)^+ \qquad \text{(II)}$$

and calculations (spin-unrestricted on $L_2Pd\bullet^+$ and R•) were performed to evaluate the energetics of these recombination

(19) Vosko, S. H.; Wilk, L.; Nusair, M. *Can. J. Phys.* **1980**, *58*, 1200.
(20) Becke, A. *Phys. Rev. A* **1988**, *38*, 3098.
(21) Perdew, J. P. *Phys. Rev. B* **1986**, *33*, 8822.
(22) Perdew, J. P. *Phys. Rev. B* **1986**, *34*, 7406.
(23) To estimate the energy of a π-coordinated imine species, costrained geometry optimizations were performed (both for the Pd−methyl and Pd−acyl species) by forcing the torsional angles Pd−N−C−H defining the position of the two H atoms bonded to the C atom of the imine to have the same absolute value. The energy of these costrained geometries with a π-coordinated imine is roughly 18−20 kcal mol^{-1} higher relative to that of the σ-coordinated species **2aP** and **2bP**.
(24) Brumbaugh, J. S.; Whittle, R. R.; Parvez, M. A.; Sen, A. *Organometallics* **1990**, *9*, 1735.

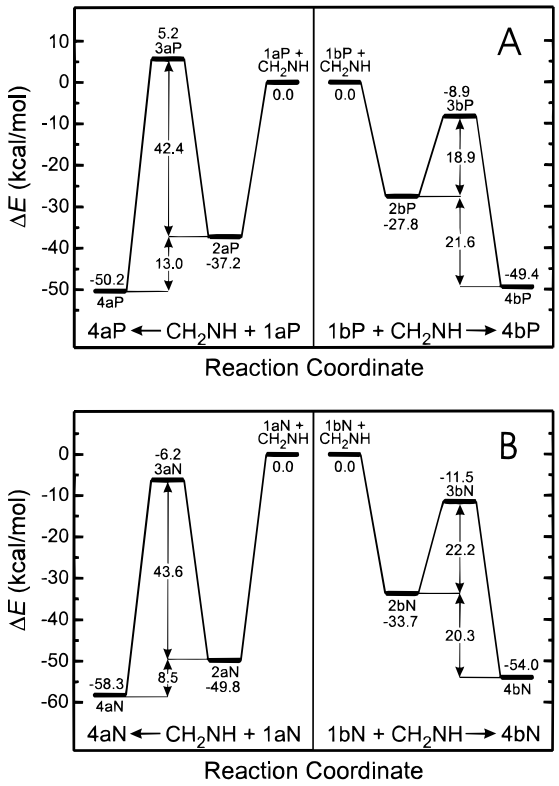

Figure 1. Reaction profiles for the imine insertion reactions with the phospane ligand, part A, and with the nitrogen-based ligand, part B. Insertion reactions into the Pd−methyl bond, **1aP 4aP** and **1aN 4aN**, are reported on the left side of parts A and B, respectively. Insertion reactions into the Pd−acyl bond, **1bP 4bP** and **1bN 4bN**, are reported on the right side of parts A and B, respectively.

reactions. Reactions I and II, and their enthalpies ΔH_{I} and ΔH_{II}, allow the breakdown of the total formation energy into contributions mainly arising from the Pd−R and from the Pd−(imine) bonds, respectively. The barriers to the insertion into the Pd−methyl and Pd−acyl bonds can thus be rewritten as:

$$\Delta H^{\ddagger} = \Delta\Delta H^{\ddagger}_{\mathrm{I}} + \Delta\Delta H^{\ddagger}_{\mathrm{II}} + \Delta H_{\mathrm{Deformation}}$$

where $\Delta\Delta H^{\ddagger}_{\mathrm{I}} = \Delta H_{\mathrm{I}}(\mathbf{3aP}) - \Delta H_{\mathrm{I}}(\mathbf{2aP})$ and $\Delta\Delta H^{\ddagger}_{\mathrm{II}} = \Delta H_{\mathrm{II}}(\mathbf{3aP}) - \Delta H_{\mathrm{II}}(\mathbf{2aP})$ for insertion into the Pd−methyl bond, while $\Delta\Delta H^{\ddagger}_{\mathrm{I}} = \Delta H_{\mathrm{I}}(\mathbf{3bP}) - \Delta H_{\mathrm{I}}(\mathbf{2bP})$ and $\Delta\Delta H^{\ddagger}_{\mathrm{II}} = \Delta H_{\mathrm{II}}(\mathbf{3bP}) - \Delta H_{\mathrm{II}}(\mathbf{2bP})$ for insertion into the Pd−acyl bond. Finally, $\Delta H_{\mathrm{Deformation}}$ represents the energy required to deform the isolated fragments $L_2Pd^{\bullet+}$, R•, and CH_2NH from the geometry they have in the reactant **2aP** or **2bP** to the geometry they have in the transition state **3aP** or **3bP**.

For insertion into the Pd−methyl bond, $\Delta\Delta H^{\ddagger}_{\mathrm{I}} = 29.8$, $\Delta\Delta H^{\ddagger}_{\mathrm{II}} = 7.9$, and $\Delta H_{\mathrm{Deformation}} = 4.7$ kcal mol^{-1}, respectively, indicating that the barrier height mainly arises from the rupture of the Pd−C(methyl) bond, which is not compensated by the formation of the new C−N bond. For insertion into the Pd−acyl bond, instead, $\Delta\Delta H^{\ddagger}_{\mathrm{I}} = 4.0$, $\Delta\Delta H^{\ddagger}_{\mathrm{II}} = 13.4$, and $\Delta H_{\mathrm{Deformation}} = 1.5$ kcal mol^{-1}, respectively, indicating that the low barrier arises from the early nature of the transition state, as indicated by the previous geometrical analysis and by the small energy loss due to the rupture of the Pd−C(acyl) bond. The driving force for the reaction stems from the formation of a strong C−N amide bond, which already at early stages of the reaction is able to drive the reaction toward the products.[25]

Finally, insertion of imine into the Pd−methyl and Pd−acyl bonds when the nitrogen-based HN═CH−CH═NH ligand is coordinated to the Pd atom was also investigated. This ligand mimics the basic skeleton of the bipyridyl ligand used by Arndtsen.[12] We begun with the following ligand substitution reaction,

$$L_2Pd(CH_3)(NCH_3)^+ + NHCH_2 \leftrightarrow L_2Pd(CH_3)(NHCH_2)^+ + NCH_3$$

with L_2 = HN═CH−CH═NH, since the L_2Pd^{II}(methyl)(imine) complexes were obtained by reacting the corresponding acetonitrile complex with imines. The ΔH we calculated for this reaction, 10.6 kcal mol^{-1}, is in very good agreement with the experimental value, 8.6 kcal mol^{-1}, obtained by Arndtsen for the ligand substitution reaction

$$(bpy)Pd(CH_3)(RN{=}C(H)Tol)^+ + CD_3CN \leftrightarrow (bpy)Pd(CH_3)(CD_3CN) + RN{=}C(H)Tol$$

with bpy = 2,2′-bipyridine, Tol = tolyl, and R = CH_3, suggesting the reliability of the adopted compuational approach.[26]

The geometries and energetics of the reactions **1aN** → **4aN** and **1bN** → **4bN** are substantially similar to the corresponding insertion reactions with the phosphane ligand. However, shorter Pd−C and Pd−N(imine) distances correspond to the more electronegative nitrogen-based ligand. For instance, the Pd−N(imine) and Pd−C(methyl) distances are 0.08 and 0.05 Å shorter in going from **2aP** to **2aN**.

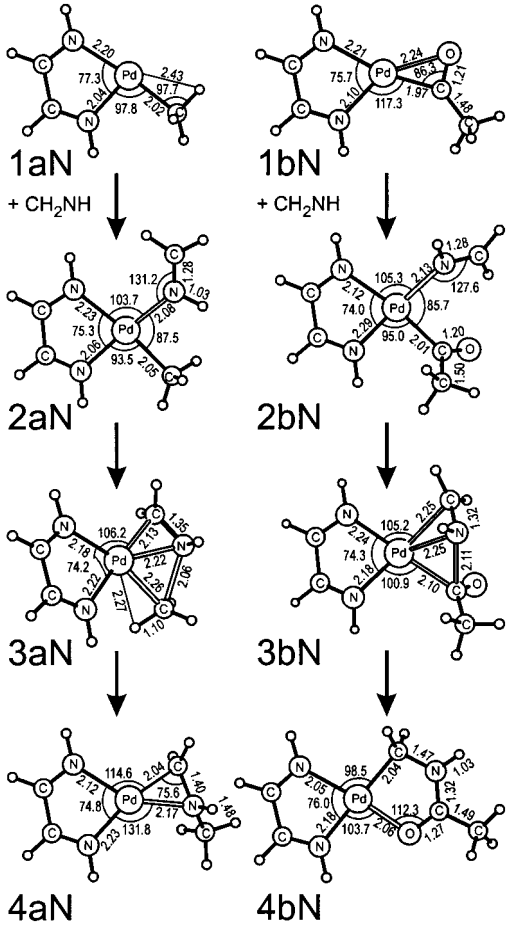

(25) The amido C−N bond is ca. 10 kcal mol^{-1} stronger than the amino C−N bond. *Handbook of Chemistry and Physics*, 74th ed.; Lide, D. R., Ed.; CRC Press Inc.: London, 1994; Vol. 74, Chapetr 9, p 145.

(26) Although imines with different R groups were investigated by Arndtsen, we think the best comparison can be obtained with the smallest R group, CH_3, since steric effects can be relevant when bulky R groups are considered.

The geometry of the product **4bN** presents the amido group forming a five-membered ring with the oxygen carbonyl atom coordinated to the Pd atom, as in the X-ray determined structure of the (bpy)Pd[C(Tol)HN(CH_3)$COCH_3$]$^+OSO_2CF_3^-$ complex. The calculated Pd−C and Pd−O distances, 2.061 and 2.038 Å, respectively, are in reasonable agreement with the experimental values, 2.008 and 2.022 Å, respectively.

The energy diagrams for the insertion reactions with the phospane and with the nitrogen-based ligands are reported in Figures 1A and 1B, respectively. The imine uptake energy to **1aN** and **1bN** is higher by 12.6 and 5.9 kcal mol^{-1} relative to **1aP** and **1bP**, respectively. However, it is worthy to note that the imine uptake energies we calculate are overestimated since we do not consider solvent and entropic effects in our calculations. Also in this case the energy barrier to the imine insertion into the Pd−methyl bond, 43.6 kcal mol^{-1}, is remarkably higher than the energy barrier to the imine insertion into the Pd−acyl bond, 22.2 kcal mol^{-1}. These values are substantially similar to the values of the corresponding insertion reactions with the phosphane-based ligand. Finally, the overall reactions **2aN** → **4aN** and **2bN** → **4bN** are exothermic with enthalpies of −8.5 and −20.3 kcal mol^{-1}, respectively.

4. Conclusions

In conclusion, we have investigated the insertion mechanism of imine into the Pd−methyl and Pd−acyl bonds with a phosphane or a nitrogen-based ligand coordinated to the Pd atom. In agreement with the experimental findings, the σ coordination of the imine is preferred. No stable geometry with a π-coordinated imine was found. However, this conclusion could depend on the absence of further substituents on the imine skeleton as well as on the substitution pattern of the phosphane ligand. The imine insertion into the Pd−methyl bond presents a high barrier, in agreement with the great kinetic stability experimentally observed for the L_2Pd(methyl)(imine) complexes. Insertion of the imine into the Pd−acyl bond, instead, occurs with a considerably lower barrier, in agreement with the experimental reactivity of the L_2Pd(acyl)(imine) complexes. A geometrical and energetic analysis of the transition states of the two insertion reactions has confirmed the hypothesis of Arndtsen and Sen, which stated that the formation of the very strong amide linkage constituted the added driving force for the imine insertion into the Pd−acyl bond.[12,13]

Acknowledgment. We thank Dr. P. Margl of Eastman Co. for fruitful discussions. This work has been supported by the Ministero della Ricerca Scientifica e Tecnologica of Italy and by Montell Polyolefins.

JA9840706